

The Layered Thiostannate (dienH₂)Cu₂Sn₂S₆: a Photoconductive Inorganic–Organic Hybrid Compound

Nicole Pienack, Angela Puls, Christian Näther, and Wolfgang Bensch*

Institute of Inorganic Chemistry, Christian-Albrechts-University of Kiel, Olshausenstrasse 40-60, 24098 Kiel, Germany

Received January 22, 2008

The new inorganic–organic hybrid compound (dienH₂)Cu₂Sn₂S₆ (dien = diethylenetriamine) was synthesized under solvothermal conditions. It crystallizes in the tetragonal space group $I4m2$ with $a = 7.8793(3)$ Å, $c = 24.9955(15)$ Å, and $V = 1551.80(13)$ Å³. The structure consists of anionic [Cu₂Sn₂S₆]²⁻ layers extending in the (001) plane and protonated amine molecules as charge compensating ions sandwiched between the layers. The layered [Cu₂Sn₂S₆]²⁻ anion is composed of a single layer of edge-sharing CuS₄ tetrahedra which is joined above and below to straight chains constructed by corner-sharing SnS₄ tetrahedra. The material is a semiconductor with an optical band gap of 1.51 eV. More interestingly, preliminary results demonstrate that the compound exhibits photoconductive properties with an increase of the conductivity by a factor of 3 when irradiated with UV light. Upon heating in an inert atmosphere the compound starts to decompose at about 256 °C.

Introduction

In recent years many efforts have been under way in the search of new and inexpensive photovoltaic materials. The materials presently used for the production of photovoltaic devices are mainly based on Si (about 90%), and thin-film materials like GaAs, amorphous Si, CdTe, or chalcopyrite compounds containing Cu, In, Ga, S, or Se¹ play only a minor but important part. Thin-film chalcogenide materials could lead to increased efficiencies and a reduction of the costs of solar cells.² A material with interesting structural and optical properties for thin-film photovoltaic applications is Cu(In,Ga)Se₂ (CIGS)^{2,3} which belongs to the group of chalcopyrites. Such quaternary chalcopyrite semiconductors can be synthesized by applying different chemical synthetic methods like chemical vapor transport or the Bridgman technique.⁴ Recently, the solvothermal synthesis of CuIn-(Se_xS_{1-x})₂ nanocrystallites was reported.⁵ During the past decade the price for indium increased dramatically. Therefore it is necessary to search for new less costly compounds with

appropriate band gaps for sunlight absorption. In addition, such materials should generate electrons and holes due to the light absorption. Combinations of different semiconductor layers establish the so-called third generation solar cells to achieve efficiencies of about 30%. Typically applied layered devices consist of materials such as semiconducting polymers and nanostructured systems.⁶

Compounds with semiconductor properties are copper-containing thiostannates (R)_xCu_aSn_bS_c (with R = organic compound) among the group of porous thiometalates. In such compounds typical properties of zeolites like gas adsorption or catalytic activity are combined with that of semiconductors or photocatalysts. Several thiostannates prepared under solvothermal conditions exhibit interesting properties.^{7–10} Two different structure types are distinguished: R-SnS-1 and R-SnS-3.^{11–14} R is an organic

* To whom correspondence should be addressed. E-mail: wbensch@ac.uni-kiel.de. Phone: +49 431 880-2419. Fax: +49 431 880-1520.

(1) Lux-Steiner, M. C.; Willeke, G. *Phys. Bl.* **2001**, *57*, 47–53.

(2) Compaan, A. D. *Sol. Energy Mater. Sol. Cells* **2006**, *90*, 2170–2180.

(3) Goetzberger, A.; Hebling, C.; Schock, H. W. *Mater. Sci. Eng.* **2003**, *R40*, 1–46.

(4) Tomm, Y.; Fiechter, S. *J. Ceram. Proc. Res.* **2005**, *6*, 141–145.

(5) Xiao, J.; Xie, Y.; Xiong, Y.; Tang, R.; Qian, Y. *J. Mater. Chem.* **2001**, *11*, 1417–1420.

(6) Barnham, K. W. J.; Mazzer, M.; Clive, B. *Nat. Mater.* **2006**, *5*, 161–164.

(7) Ahari, H.; Bowes, C. L.; Jiang, T.; Lough, A.; Ozin, G. A.; Bedard, R. L.; Petrov, S.; Young, D. *Adv. Mater.* **1995**, *7*, 375–377.

(8) Ahari, H.; Ozin, G. A.; Bedard, R. L.; Petrov, S.; Young, D. *Adv. Mater.* **1995**, *7*, 370–374.

(9) Enzel, P.; Henderson, G. S.; Ozin, G. A.; Bedard, R. L. *Adv. Mater.* **1995**, *7*, 64–68.

(10) Jiang, T.; Ozin, G. A.; Bedard, R. L. *Adv. Mater.* **1995**, *7*, 166–170.

(11) Jiang, T.; Lough, A.; Ozin, G. A. *Adv. Mater.* **1998**, *10*, 42–46.

(12) Parise, J. B.; Ko, Y.; Rijssenbeek, J.; Nellis, D. M.; Tan, K.; Koch, S. *J. Chem. Soc., Chem. Commun.* **1994**, 527.

(13) Ko, Y.; Tan, K.; Nellis, D. M.; Koch, S.; Parise, J. B. *J. Solid State Chem.* **1995**, *114*, 506–511.

component acting as a structure directing molecule. The structures are composed of two-dimensional anionic layers with compositions $[\text{Sn}_3\text{S}_7]^{2-}$ and $[\text{Sn}_4\text{S}_9]^{2-}$ for R-SnS-1 and R-SnS-3, respectively. In R-SnS-1 the primary building units (PBUs) are SnS_4 tetrahedra which are combined to form Sn_3S_4 semicubes as secondary building units (SBUs). Two S^{2-} anions connect the semicubes to form the anionic layers $[\text{Sn}_3\text{S}_7]^{2-}$ with pores consisting of 24 atoms (diameter: $10 \text{ \AA} \times 10 \text{ \AA}$). The organic components, like for example, tetraethylammonium, act as charge compensating cations and are located below/above the pores between the layers.¹⁵ In R-SnS-3 the SBUs are joined by SnS_4 tetrahedra to form $[\text{Sn}_4\text{S}_9]^{2-}$ anionic layers. The pores are elliptical with a size of about $13 \text{ \AA} \times 15 \text{ \AA}$.¹⁴ Instead of organic structure directors alkali metals were used to prepare 2D compounds like $\text{Rb}_2\text{Sn}_3\text{S}_7 \cdot 2\text{H}_2\text{O}$ or $\text{Cs}_4\text{Sn}_5\text{S}_{12} \cdot 2\text{H}_2\text{O}$.^{16,17}

Many compounds prepared under solvothermal conditions have been studied in recent years, but most of them are wide band gap semiconductors. Thiostannates are candidates for catalytic applications, chemical sensing,^{11,12,18–20} and with the integration of transition metals (TM) into the network the physical and chemical properties are altered.²¹ Some TM containing thiostannates were reported until now,^{21–24} and we recently presented two new compounds with copper integrated into the thiostannate network.²⁵ The promising photochemical properties of Cu and Sn containing sulfides were demonstrated recently on the substitution series $\text{Cu}_2\text{Sn}_{1-x}\text{Si}_x\text{S}_3$ ²⁶ which were prepared using the classical high temperature route. The results of this study motivated us to perform syntheses with Cu, Sn, and S applying an amine as structure director. One goal of the experiments is the search for materials where the rare indium is replaced by tin exhibiting potential photovoltaic properties. In this paper we present the synthesis, crystal structure, and selected properties of the new thiostannate $(\text{dienH}_2)\text{Cu}_2\text{Sn}_2\text{S}_6$ (dien = diethylenetriamine, $\text{C}_4\text{N}_3\text{H}_{13}$). We also report the first results of experiments concerning photoconductive properties of the compound.

Table 1. Selected Details of Data Collection and Results of the Refinement of $(\text{dienH}_2)\text{Cu}_2\text{Sn}_2\text{S}_6$

compound	$(\text{dienH}_2)\text{Cu}_2\text{Sn}_2\text{S}_6$
crystal system	tetragonal
space group	$I\bar{4}m2$
$a/\text{\AA}$	7.8793(3)
$b/\text{\AA}$	7.8793(3)
$c/\text{\AA}$	24.9955(15)
$V/\text{\AA}^3$	1551.80(13)
Z	4
$D_{\text{calculated}}/\text{g/cm}^3$	2.834
μ/mm^{-1}	6.673
scan range	$2.71 \leq \theta \leq 28.03^\circ$
reflections collected	6243
refl. with $F_o > 4\sigma(F_o)$	1256
independent reflections	1078
goodness-of-fit on F^2	1.052
final R indices [$I > 2\sigma(I)$]	R1 = 0.0417, wR2 = 0.0979
R indices (all data)	R1 = 0.0471, wR2 = 0.1018
res. elec. dens./ \AA^{-3}	3.923/–1.949
Flack x parameter	0.02(6)

Experimental Details

Synthesis. General Information. All reactions were performed under solvothermal conditions in Teflon-lined steel autoclaves (inner volume, 30 mL). The crystalline products were filtered off after the reactions, washed with water and ethanol, and dried in vacuum.

Synthesis of $(\text{dienH}_2)\text{Cu}_2\text{Sn}_2\text{S}_6$. A 0.5 mmol portion of Sn (99.5%, Aldrich), 0.5 mmol of Cu (99.5%, Alfa Aesar), 2 mmol of S, and 6 mL of diethylenetriamine ($\geq 97.0\%$, Fluka) were heated to $170 \text{ }^\circ\text{C}$ in 2 h and then reacted for 120 h at this temperature, followed by cooling to $25 \text{ }^\circ\text{C}$ in 30 h. The synthesis was performed in a diffusion cell to separate Cu from Sn and S by a membrane. The advantage of such a cell is that the dissolved Sn and Cu species must diffuse through the membrane keeping the concentration of the reacting species low at the site of crystallization. Thin black plates of the title compound were obtained in 15% yield based on Sn, which were slightly contaminated with sulfides on the surface. Performing the synthesis under stirring, we received the black powder in a 60% yield (based on Sn). The composition was confirmed by EDX (Sn/Cu/S ratio, 1:1:3) and by elemental analysis (results in %; found: C 7.29, H 2.05, N 6.04; calculated: C 7.23, H 2.58, N 6.33).

Structure Determination. Intensity data were collected using a STOE IPDS-1 (Imaging Plate Diffraction System) with Mo K α radiation at room temperature. The structure was solved with direct methods using the program SHELXS-97²⁷ and the refinement was done against F^2 with SHELXL-97.²⁸ All atoms except H were refined with anisotropic displacement parameters. The dienH₂ molecule is located on a crystallographic mirror plane with the nitrogen atom N2 disordered over two positions. The N–H and the C–H hydrogen atoms were positioned with idealized geometry and were refined using a riding model with $U_{\text{eq}}(\text{H}) = 1.2$ or $1.5 U_{\text{eq}}(\text{C,N})$. Crystal data and selected refinement results are summarized in Table 1. Further structural details have been deposited with the Cambridge Crystallographic Data Centre (CCDC) as publication no. CCDC 701160 (I). Copies of the data can be obtained, free of charge, on application to CCDC, 12 Union Road, Cambridge CB2 1EZ, U.K. (mail: deposit@ccdc.ca.ac.uk).

Thermal Investigations. Differential thermal analysis-thermogravimetry (DTA-TG) analyses were performed using a Netzsch STA 429 DTA-TG device. The samples were heated to $600 \text{ }^\circ\text{C}$ at

- (14) Jiang, T.; Lough, A.; Ozin, G. A.; Bedard, R. L.; Broach, R. J. *Mater. Chem.* **1998**, *8*, 721–732.
- (15) Jiang, T.; Lough, A.; Ozin, G. A.; Bedard, R. L. *J. Mater. Chem.* **1998**, *8*, 733–741.
- (16) Jiang, T.; Ozin, G. A.; Bedard, R. L. *J. Mater. Chem.* **1998**, *8*, 1641–1648.
- (17) Sheldrick, W. S.; Schaaf, B. Z. *Anorg. Allg. Chem.* **1994**, *620*, 1041–1045.
- (18) Scott, R. W. J.; MacLachlan, M. J.; Ozin, G. A. *Curr. Opin. Solid State Mater. Sci.* **1999**, *4*, 113–121.
- (19) Jiang, T.; Ozin, G. A. *J. Mater. Chem.* **1997**, *7*, 2213–2222.
- (20) Francis, R. J.; Price, S. J.; Evans, J. S. O.; O'Brien, S.; O'Hare, D.; Clark, S. M. *Chem. Mater.* **1996**, *8*, 2102–2108.
- (21) An, Y.; Ji, M.; Baiyin, M.; Liu, X.; Jia, C.; Wang, D. *Inorg. Chem.* **2003**, *14*, 4248–4249.
- (22) Palchik, O.; Iyer, R. G.; Liao, J. H.; Kanatzidis, M. G. *Inorg. Chem.* **2003**, *42*, 5052–5054.
- (23) Dag, Ö.; Ahari, H.; Coombs, N.; Jiang, J.; Aroca-Quellette, P. P.; Petrov, S. *Adv. Mater.* **1997**, *9*, 1133–1149.
- (24) Bowes, C. L.; Petrov, S.; Vovk, G.; Young, D.; Ozin, G. A.; Bedard, R. L. *J. Mater. Chem.* **1998**, *8*, 711–720.
- (25) Pienack, N.; Näther, C.; Bensch, W. *Solid State Sci.* **2007**, *9*, 100–107.
- (26) Lafond, A.; Cody, J. A.; Souilah, M.; Guillot-Deudon, C.; Kiebach, R.; Bensch, W. *Inorg. Chem.* **2007**, *46*, 1502–1506, vorher.

- (27) Sheldrick, G. M. *SHELXS 97, Program for the Solution of Crystal Structures*; University of Göttingen: Göttingen, Germany, 1997.
- (28) Sheldrick, G. M. *SHELXL 97, Program for the Refinement of Crystal Structures*; University of Göttingen: Göttingen, Germany, 1997.

a rate of $4 \text{ K} \cdot \text{min}^{-1}$ under a flow of argon ($75 \text{ mL} \cdot \text{min}^{-1}$) in Al_2O_3 crucibles. The TG-MS measurements with a heating rate of $4 \text{ K} \cdot \text{min}^{-1}$ in Al_2O_3 crucibles and in a dynamic helium atmosphere with a flow rate of $75 \text{ mL} \cdot \text{min}^{-1}$ were conducted simultaneously using a STA-409CD device (Netzsch) with Skimmer coupling, which is equipped with a Balzers QMA 400 Quadrupole Mass Spectrometer (max. 512 amu). The MS data were recorded in the analogue and trend scan modes. The TG data were corrected for buoyancy and current effects. An isothermal experiment was performed at $150 \text{ }^\circ\text{C}$ for 5 h in Ar atmosphere.

Spectroscopic Experiments. Raman. The Raman spectra were recorded in the region from 100 to 3500 cm^{-1} with a Bruker IFS 66 Fourier Transform Raman spectrometer (wavelength: 541.5 nm).

UV/vis. UV/vis spectroscopic investigations were conducted at room temperature using a UV-vis-NIR two-channel spectrometer Cary 5 from Varian Techtron Pty., Darmstadt. The optical properties of the compound were investigated by studying the UV/vis reflectance spectrum of a powdered sample. The absorption data were calculated with the Kubelka–Munk relation for diffuse reflectance data. BaSO_4 powder was used as reference material.

Scanning Electron Microscopy (SEM)/Energy Dispersive X-ray Fluorescence (EDX). The EDX analyses have been carried out with a Philips ESEM XL30 equipped with an EDAX detector.

Elemental Analysis. CHNS analyses were done using a EURO EA Elemental Analyzer, fabricated by EURO VECTOR Instruments and Software.

Impedance Spectroscopy. The impedance measurements were done on a pressed pellet with the so-called “Kieler cell” in argon atmosphere using a HP 4192 Impedance-Analyzer at 5 – 13 MHz with gold electrodes. The temperature was controlled with a Cr/CrNi thermocouple. The equivalent circuit diagram contains a resistance (R) and a capacitance (C) in parallel. The resulting semicircle, the so-called Nyquist plot, has a high frequency limit at the origin and a low frequency limit at $Z' = R$. The values for the resistance from the Nyquist plot were converted using the dimensions of the pressed pellet ($d = 0.55 \text{ mm}$, area = 50.3 mm^2) to obtain the values for the resistivity. The capacitance could be obtained from the maximum of the semicircle. For the photoconductivity measurements a UV lamp ($\lambda = 300$ – 400 nm) was used.

Results and Discussion

Crystal Structures. The new compound $(\text{dienH}_2)\text{Cu}_2\text{Sn}_2\text{S}_6$ crystallizes in the non-centrosymmetric tetragonal space group $I\bar{4}m2$ with 4 formula units in the unit cell. All non-H atoms are located on special positions. The structure consists of anionic $[\text{Cu}_2\text{Sn}_2\text{S}_6]^{2-}$ layers which are separated by the charge compensating cations, that is, the protonated amine molecules. The two crystallographically independent Sn atoms and the Cu atom are in a tetrahedral environment of S atoms (Figure 1).

SnS_4 tetrahedra are common in thioantimonates and the observed Sn–S distances ($2.357(2)$ – $2.486(3) \text{ \AA}$, Table 2) as well as the S–Sn–S angles ($103.59(11)$ – $117.98(10)^\circ$, Table 2) indicate a slight distortion.

The geometric parameters are in good agreement with data published in the literature.^{16,29,30} The Cu–S bond lengths in the CuS_4 tetrahedron are $2.3464(13)$ and $2.3555(12) \text{ \AA}$,

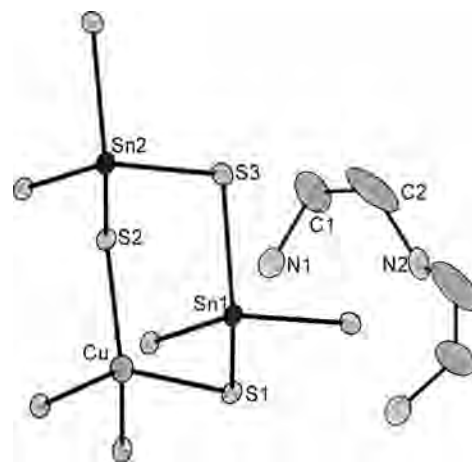


Figure 1. Connection of the SnS_4 and CuS_4 tetrahedra together with the amine molecule and labeling of the atoms of the asymmetric unit. The displacement ellipsoids are drawn at the 50% probability level. The hydrogen atoms and the disorder of N2 are not shown for clarity.

Table 2. Selected Bond Lengths and Angles of (I)^a

Sn(1)–S(1)	2.357(2)	S(2)–Sn(2)–S(3)	107.44(4)
Sn(1)–S(3)	2.485(3)	S(3)–Sn(2)–S(3) ^f	106.13(12)
Sn(2)–S(2)	2.359(2)	S(2)–Cu–S(2) ^d	113.04(11)
Sn(2)–S(3)	2.486(3)	S(2)–Cu–S(1) ^e	106.61(7)
Cu–S(2)	2.3464(13)	S(2)–Cu–S(1)	113.88(5)
Cu–S(1)	2.3555(12)	S(2) ^d –Cu–S(1)	106.61(7)
S(1)–Cu ^f	2.3555(12)	S(1) ^e –Cu–S(1)	102.51(11)
S(2)–Cu ^g	2.3464(13)	Cu–S(1)–Cu ^f	116.43(8)
		Cu–S(1)–Sn(1)	103.93(6)
S(1)–Sn(1)–S(1) ^b	117.98(10)	Cu ^g –S(2)–Cu	111.32(8)
S(1)–Sn(1)–S(3)	108.58(4)	Cu–S(2)–Sn(2)	103.95(6)
S(3) ^b –Sn(1)–S(3)	103.59(11)	Sn(1)–S(3)–Sn(2)	104.86(8)
S(2)–Sn(2)–S(2) ^c	120.16(11)		

^a The symmetry transformations used to generate equivalent atoms are indicated in the footnotes. ^b $-x, -y, z$. ^c $-x + 1, -y, z$. ^d $-y + 1/2, x - 1/2, -z + 1/2$. ^e $-y + 1/2, x + 1/2, -z + 1/2$. ^f $y - 1/2, -x + 1/2, -z + 1/2$. ^g $y + 1/2, -x + 1/2, -z + 1/2$.

being longer than in CuInS_2 ³¹ but similar to values observed in the compounds presented below. The S–Cu–S angles vary between $102.51(11)$ and $113.88(5)^\circ$ indicating a pronounced distortion of the tetrahedron. Such a distortion is not uncommon, and similar values were reported in the literature. For instance, in the compounds Rb_2CuMS_4 ($M = \text{Nb}, \text{V}$)³² linear chains are constructed by edge-sharing of CuS_4 and MS_4 tetrahedra and also in RbCu_2VS_4 Cu is in a distorted tetrahedral environment.³³ Analyzing the structures of different thiometalates the occurrence of CuS_4 tetrahedra in copper thioantimonates is quite unusual, whereas in Cu thioantimonates CuS_4 tetrahedra are more common like, for example, $(\text{C}_4\text{N}_3\text{H}_{14})\text{Cu}_3\text{Sb}_2\text{S}_5$ ($\text{C}_4\text{N}_3\text{H}_{13}$ = diethylenetriamine) and $(\text{C}_6\text{N}_4\text{H}_{20})_{0.5}\text{Cu}_3\text{Sb}_2\text{S}_5$ ($\text{C}_6\text{N}_4\text{H}_{18}$ = triethylenetetramine).³⁴

All S atoms of the CuS_4 tetrahedron share a corner with neighboring CuS_4 tetrahedra to form a single puckered layer $[\text{CuS}_{4/4}]$ within the (001) plane containing Cu_4S_4 rings as a special structural feature (Figure 2, bottom).

(31) Hahn, H.; Frank, G.; Klingler, W.; Meyer, A. D.; Stoerger, G. *Z. Anorg. Allg. Chem.* **1953**, *271*, 153.

(32) Rumpf, C.; Tillinski, R.; Näther, C.; Dürichen, P.; Jess, I.; Bensch, W. *Eur. J. Solid State Inorg. Chem.* **1997**, *34*, 1187–1198.

(33) Tillinski, R.; Näther, C.; Bensch, W. *Acta Crystallogr.* **2001**, *C57*, 333–334.

(34) Spetzler, V.; Näther, C.; Bensch, W. *Inorg. Chem.* **2005**, *44*, 5805–5812.

(29) Behrens, M.; Scherb, S.; Näther, C.; Bensch, W. *Z. Anorg. Allg. Chem.* **2003**, *629*, 1367–1373.

(30) Jiang, T.; Ozin, G. A. *J. Mater. Chem.* **1998**, *8*, 1099–1108.

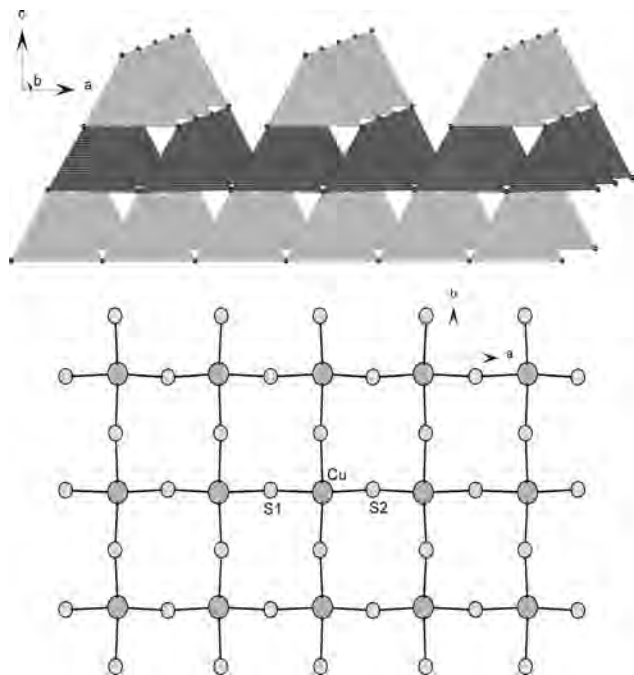


Figure 2. Polyhedral representation of the layered $[\text{Cu}_2\text{Sn}_2\text{S}_6]^{2-}$ anion (top: SnS_4 tetrahedra light gray and CuS_4 tetrahedra dark gray) and a layer in the (001) plane formed by corner-sharing of CuS_4 tetrahedra (bottom).

The different positions of the Sn atoms ($\text{Sn}(1)$ and $\text{Sn}(2)$) do not correspond neither to two different sheets nor to different chains. The $\text{Sn}(1)\text{S}_4$ and $\text{Sn}(2)\text{S}_4$ tetrahedra are joined via common corners into one-dimensional chains $[\text{SnS}_{4/2}]$ running along [100] and [010]. The chains are bound to the $[\text{CuS}_{4/4}]$ layer via S(1) and S(2) yielding the layered $[\text{Cu}_2\text{Sn}_2\text{S}_6]^{2-}$ anion (Figure 2, top). As a consequence of the connection mode the two atoms S(1) and S(2) have bonds to two Cu and one Sn centers whereas S(3) is only bound to two Sn atoms. The Cu–Sn distances are about 3.7 Å which are too long for any significant interactions.

The layers are stacked perpendicular to [001] with the protonated amine molecules residing in the void space with neighboring amines being rotated by 90° (Figure 3).

The terminal N(1) atom has two contacts to S atoms (3.292 Å to S(1) and 3.275 Å to S(2)) indicating weak $\text{N}(1)\text{---H}\cdots\text{S}$ bonding interactions. The shortest interlayer distance of 5.3 Å is determined by the arrangement of the organic molecules.

From a formal point of view the title compound belongs to a group of compounds with general composition $\text{M}_2^{\text{I}}\text{M}^{\text{IV}}\text{Q}_3$ with $\text{M}^{\text{I}} = \text{Cu}$, $\text{M}^{\text{IV}} = \text{Si}$, Ge , Sn and $\text{Q} = \text{S}$, Se .^{35–39} and $\text{K}_2\text{MM}'_3\text{Se}_6$ ($\text{M} = \text{Cu}$, Ag ; $\text{M}' = \text{Ga}$, In).⁴⁰ The structures of the members of the $\text{M}_2^{\text{I}}\text{M}^{\text{IV}}\text{Q}_3$ series can be viewed as derivatives of the cubic sphalerite type structure, that is, the

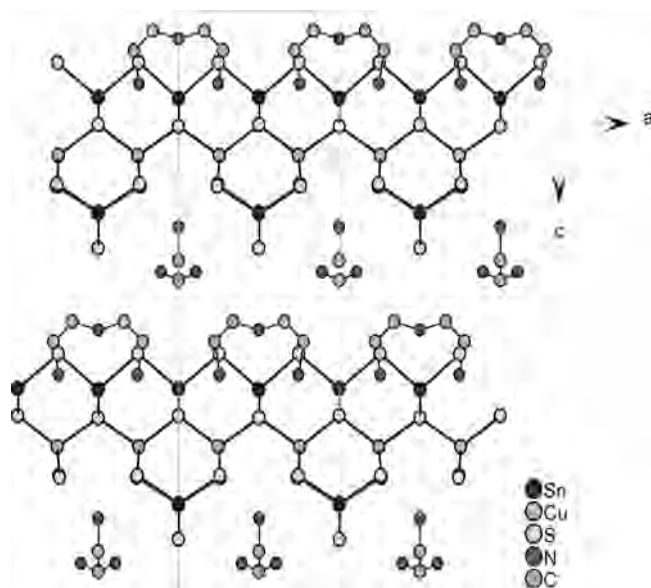


Figure 3. Arrangement of the $[\text{Cu}_2\text{Sn}_2\text{S}_6]^{2-}$ layers and the amine molecules in the interlayer galleries. The hydrogen atoms are omitted for clarity.

tetrahedra form a three-dimensional network. The structures of the latter series of compounds are layered. A sublayer is composed by InS_4 and CuS_4 tetrahedra sharing all four corners leading to a topology which is similar to that of the title compound. This sublayer is sandwiched by parallel corner-sharing $[\text{InS}_4]$ tetrahedral chains. Another structurally related compound is $\text{Rb}_2\text{Cu}_2\text{Sn}_2\text{S}_6$ ⁴¹ which may be regarded as a derivative of the $\text{M}_2^{\text{I}}\text{M}^{\text{IV}}\text{Q}_3$ structure by substituting one Cu^+ by a Rb^+ ion yielding a layered structure. In this structure a layer constructed by corner-sharing CuS_4 tetrahedra is sandwiched by two layers composed of SnS_4 tetrahedra. In the two Sn containing layers 1/2 of the Sn sites are empty so that chains are formed running perpendicularly below and above the Cu layer. The interlayer separation in $\text{Rb}_2\text{Cu}_2\text{Sn}_2\text{S}_6$ amounts to 4.8 Å which is shorter than in the title compound.

Spectroscopy. Charge neutrality of the title compound requires that the amine molecule is diprotonated. In diethylenetriamine usually the primary amino groups are protonated. In this case, the IR spectra show the absorptions located at 1530, 1630, and 3430 cm^{-1} which are excited by R-NH_3^+ groups.

In the Raman spectrum (Figure 4) vibrations occur at 373, 301, 267, and 233 cm^{-1} which is the typical region for Sn–S resonances.^{42,43} The symmetric Sn–S stretching vibration is located at 373 cm^{-1} and a symmetric Sn–S bridging mode at 301 cm^{-1} . The signal at 233 cm^{-1} could be assigned to the SnS_2 wagging and twisting mode, and the resonance at 267 cm^{-1} is caused by Cu–S vibrations.⁴⁴

The optical band gap E_g was determined from transformed UV/vis diffuse reflectance spectra by the Kubelka–Munk method. The value of 1.51 eV (821 nm, Figure 5) is in agreement with the black color of the crystals. The band gap

- (35) Chen, X. A.; Wada, H.; Sato, A.; Nozaki, H. *J. Alloys Compd.* **1999**, *290*, 91–96.
 (36) Marcano, G.; Rincon, C.; Chalbaud, L. M. de; Brando, D. B.; Sanchez Perez, G. *J. Appl. Phys.* **2001**, *90*, 1847–1853.
 (37) Delgado, G. E.; Mora, A. J.; Marcona, G.; Rincon, C. *Mater. Res. Bull.* **2003**, *38*, 1949–1955.
 (38) Onoda, M.; Chen, X. A.; Sato, A.; Wada, H. *Mater. Res. Bull.* **2000**, *35*, 1563–1570.
 (39) Chalbaud, L. M. de; Delgado, G. Diaz de; Delgado, J. M.; Mora, A. E.; Sagredo, V. *Mater. Res. Bull.* **1997**, *32*, 1371–1376.
 (40) Ma, H.-W.; Guo, G. C.; Wang, M.-S.; Zhou, G.-W.; Lin, S.-H.; Dong, Z.-C.; Huang, J.-S. *Inorg. Chem.* **2003**, *42*, 1366–1370.

- (41) Liao, J.-H.; Kanatzidis, M. G. *Chem. Mater.* **1993**, *5*, 1561–1569.
 (42) Krebs, B.; Schiwy, W. *Z. Anorg. Allg. Chem.* **1973**, *398*, 63–71.
 (43) Krebs, B.; Pohl, S.; Schiwy, W. *Angew. Chem.* **1970**, *82*, 884–885.
 (44) Müller, A.; Menge, R. *Z. Anorg. Allg. Chem.* **1972**, *393*, 259–265.

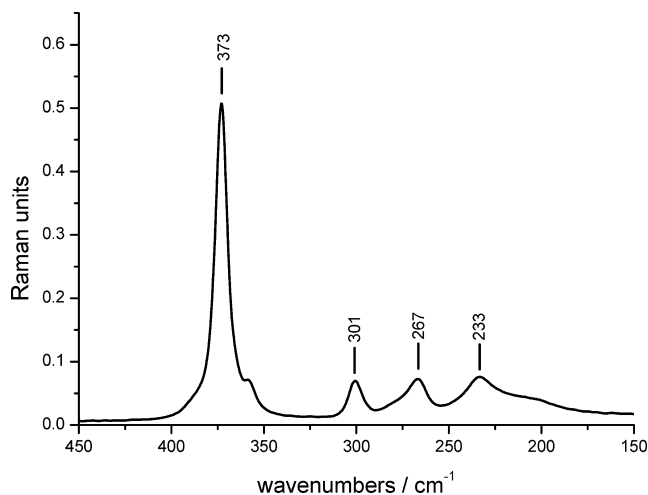


Figure 4. Raman spectrum of $(\text{dienH}_2)\text{Cu}_2\text{Sn}_2\text{S}_6$ with the centers of the resonances given in cm^{-1} .

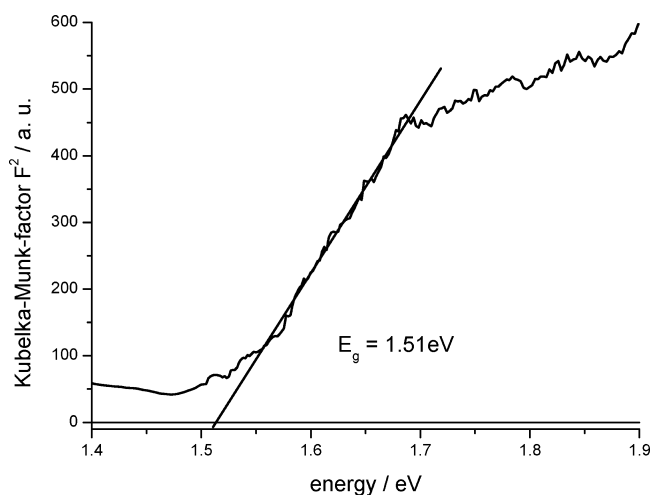


Figure 5. Determination of the optical band gap of $(\text{dienH}_2)\text{Cu}_2\text{Sn}_2\text{S}_6$ from UV/vis diffuse reflectance spectrum using the Kubelka–Munk method.

of the title compound is comparable to that of CdTe (1.5 eV) or GaAs (1.4 eV) which are together with CIS or CIGS (copper indium gallium selenide) efficient photovoltaic materials.^{45,46} We note that the value for E_g of $(\text{dienH}_2)\text{Cu}_2\text{Sn}_2\text{S}_6$ is slightly larger than that for the structurally related compound $\text{Rb}_2\text{Cu}_2\text{Sn}_2\text{S}_6$ which was reported to be 1.44 eV.⁴¹ Plotting $((\alpha/S) \cdot E)^2$ versus the energy (α/S) is the Kubelka–Munk factor) shows a linear behavior so that the band gap can be assumed to be direct.⁴¹

Thermo Analytical Measurements. The DTA-TG-DTG and MS trend scan curves are shown in Figure 6. The compound starts to decompose at $T_{\text{onset}} = 256^\circ\text{C}$ with an endothermic signal at $T_p = 262^\circ\text{C}$. TG-MS investigations show that the amine and H_2S are emitted simultaneously at the decomposition temperature. The total weight loss of 23.5% is slightly lower than the calculated value for the emission of the amine and two H_2S molecules ($-\Delta m_{\text{theo}} = 25.7\%$). The residue is black and contains nearly 2% of CHN. In the X-ray powder pattern of the residue the compounds SnS and Cu_2SnS_3 could be identified.

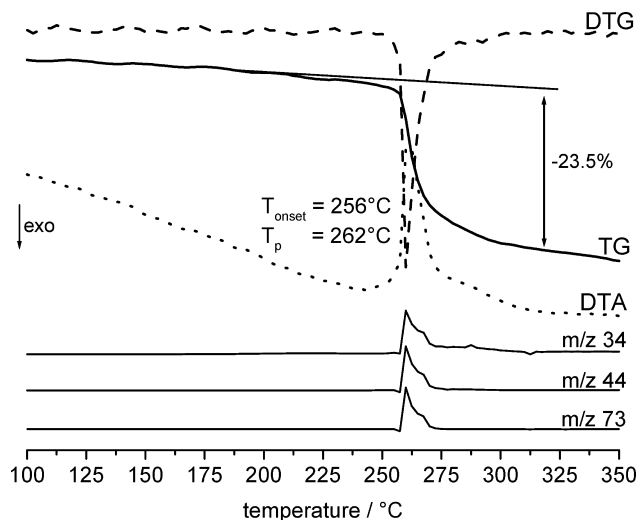


Figure 6. DTA-TG-MS trend scan curves of $(\text{dienH}_2)\text{Cu}_2\text{Sn}_2\text{S}_6$. Intensities of the signals are in arbitrary units, m/z 34 = H_2S ; m/z 44 and m/z 73 are fragments of diethylenetriamine.

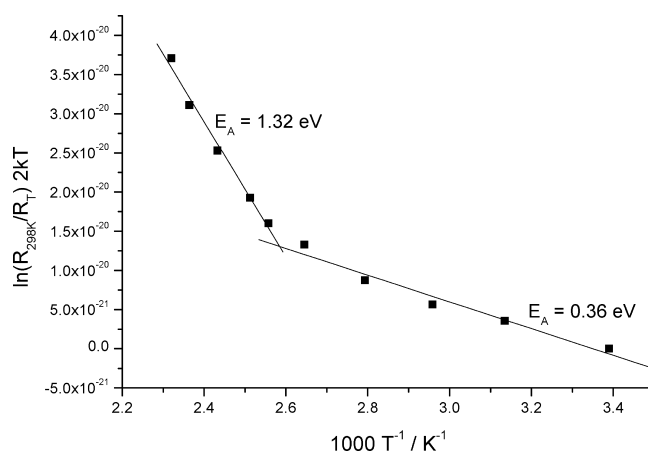


Figure 7. Arrhenius plot displaying two different regions for the activation energy (for details, see text).

An isothermal experiment performed for 5 h at 150°C in Ar atmosphere exhibits a very small mass loss of about 2%. The X-ray powder pattern recorded after this experiment shows only the reflections of the title compound. In addition, chemical analysis (6.1% N, 7.3% C, and 2.1% H) gives no hints for a significant decomposition, and we therefore assume that surface water was emitted.

Impedance Spectroscopy. The resistivity, the conductivity, and the capacitance at room temperature were estimated from the Nyquist plot as $R_{\text{RT}} = 7.22 \times 10^6 \Omega \cdot \text{cm}$, $\sigma_{\text{RT}} = 1.38 \times 10^{-7} \Omega^{-1} \text{cm}^{-1}$, and $C_{\text{RT}} = 0.135 \text{ nF}$. The resistivity decreases with increasing temperature reaching $3.02 \times 10^5 \Omega \cdot \text{cm}$ at 158°C .

Applying the Arrhenius equation the activation energy was determined as $E_A = 0.36 \text{ eV}$ for the extrinsic and $E_A = 1.32 \text{ eV}$ for the intrinsic conductivity (Figure 7). Impurities or point defects in the material could explain the discrepancy between the optical band gap and the activation energy determined with impedance spectroscopy.

Exposing the material to UV light for some minutes leads to a strong decrease of the resistivity (Figure 8) exhibiting the difference between the dark and the photo current. After

(45) Miles, R. W.; Zoppi, G.; Forbes, I. *Mater. Today* **2007**, *10*, 20–27.

(46) Conibeer, G. *Mater. Today* **2007**, *10*, 42–50.

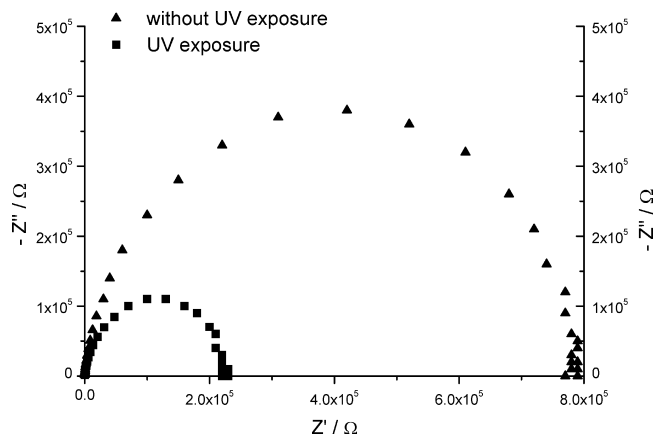


Figure 8. Nyquist plots from impedance measurements showing the resistance with and without UV light exposure.

20 min exposure a minimum of $R_{UV} = 2.01 \times 10^6 \Omega \cdot \text{cm}$ was reached, and further irradiation with UV light does not change the resistivity. The increase of the conductivity is larger than a factor of 3. After switching-off the UV irradiation the resistivity increased to $7.22 \times 10^6 \Omega \cdot \text{cm}$ which is the value measured without UV light.

Conclusions

The new copper thiostannate $(\text{dienH}_2)\text{Cu}_2\text{Sn}_2\text{S}_6$ was obtained as thin black plates under solvothermal conditions. Under static conditions the yield is low but can be increased by a factor of 4 by stirring the starting mixture. The structure is constructed by alternate stacking of $[\text{Cu}_2\text{Sn}_2\text{S}_6]^{2-}$ layers and protonated amine molecules. The structural motif of the anionic layer is related to a series of compounds with compositions $\text{M}_2^{\text{I}}\text{M}^{\text{IV}}\text{Q}_3$ with $\text{M}^{\text{I}} = \text{Cu}$, $\text{M}^{\text{IV}} = \text{Si}$, Ge , Sn and $\text{Q} = \text{S}$, Se and $\text{K}_2\text{MM}'_3\text{Se}_6$ ($\text{M} = \text{Cu}$, Ag ; $\text{M}' = \text{Ga}$, In). All these compounds contain only inorganic constituents. Replacement of a part of the small M^{I} ions by the protonated

dien molecule yields an inorganic–organic hybrid compound exhibiting an inorganic substructure very similar to that observed in the other compounds. The preliminary results of the impedance measurements evidence the semiconducting character of the title compound with a band gap typical for photoconductors. First experiments indicate that the electrical properties of the compound can be influenced by irradiating the material with UV light leading to a reduction of the resistivity by a factor of 3. Recently, we demonstrated that the optical band gap of $\text{Cu}_2\text{Sn}_{1-x}\text{Si}_x\text{S}_3$ can be altered from 1.25 to 1.45 eV through a substitution of Sn by Si.²⁶ For the title compound challenging questions are whether the material can be prepared applying different amines and how these organic molecules influence the electric properties. In addition, doping experiments are necessary to alter the conductivity of the compound, that is, a distinct doping level would allow controlling the conductivity. Such experiments are currently under way. Copper thiostannates are flexible with respect to the crystal structure and the chemical composition, and it can be assumed that more Cu/Sn based inorganic–organic hybrid compounds are accessible using different synthesis conditions. Further studies are needed to elucidate whether the compound is a candidate for further applications.

Acknowledgment. We thank Dr. C. Knittlmayer and Prof. Dr. W. Weppner (Tech. Faculty, University of Kiel) for the possibility and their help during the impedance measurements. We also thank Dr. G. Popkirov (Tech. Faculty, University of Kiel) for fruitful discussions about photovoltaic materials.

Supporting Information Available: X-ray crystallographic file (in CIF format) of the title compound. This material is available free of charge via the Internet at <http://pubs.acs.org>.

IC800118Z